British Journal of Pharmacology (2007) 151, 332–340
 0007–1188/07 $30.00
www.brjpharmacol.org

RESEARCH PAPER

Effects of methyl β-cyclodextrin on EDHF responses in pig and rat arteries; association between SK_{Ca} channels and caveolin-rich domains

M Absi[1,3], MP Burnham[1,3], AH Weston[1], E Harno[1], M Rogers[2] and G Edwards[1]

[1]*Faculty of Life Sciences, University of Manchester, Core Technology Facility, Manchester, UK and* [2]*Imaging Science and Biomedical Engineering, The University of Manchester, Manchester, UK*

Background and purpose: The small and intermediate conductance, Ca^{2+}-sensitive K^+ channels (SK_{Ca} and IK_{Ca}, respectively) which are pivotal in the EDHF pathway may be differentially activated. The importance of caveolae in the functioning of IK_{Ca} and SK_{Ca} channels was investigated.
Experimental approach: The effect of the caveolae-disrupting agent methyl-β-cyclodextrin (MβCD) on IK_{Ca} and SK_{Ca} localization and function was determined.
Key results: EDHF-mediated, SK_{Ca}-dependent myocyte hyperpolarizations evoked by acetylcholine in rat mesenteric arteries (following blockade of IK_{Ca} with TRAM-34) were inhibited by MβCD. Hyperpolarizations evoked by direct SK_{Ca} channel activation (using NS309 in the presence of TRAM-34) were also inhibited by MβCD, an effect reversed by cholesterol. In contrast, IK_{Ca}-dependent hyperpolarizations (in the presence of apamin) were unaffected by MβCD. Similarly, in porcine coronary arteries, EDHF-mediated, SK_{Ca}-dependent (but not IK_{Ca}-dependent) endothelial cell hyperpolarizations evoked by substance P were inhibited by MβCD. In mesenteric artery homogenates subjected to sucrose-density centrifugation, caveolin-1 and SK3 (SK_{Ca}) proteins but not IK1 (IK_{Ca}) protein migrated to the buoyant, caveolin-rich fraction. MβCD pretreatment redistributed caveolin-1 and SK3 proteins into more dense fractions. In immunofluorescence images of porcine coronary artery endothelium, SK3 (but not IK1) and caveolin-1 were co-localized. Furthermore, caveolin-1 immunoprecipitates prepared from native porcine coronary artery endothelium contained SK3 but not IK1 protein.
Conclusions and Implications: These data provide strong evidence that endothelial cell SK_{Ca} channels are located in caveolae while the IK_{Ca} channels reside in a different membrane compartment. These studies reveal cellular organisation as a further complexity in the EDHF pathway signalling cascade.
British Journal of Pharmacology (2007) **151,** 332–340; doi:10.1038/sj.bjp.0707222; published online 23 April 2007

Keywords: caveolae; EDHF; calcium-activated potassium channels; NS309; apamin; TRAM-34

Abbreviations: ACh, acetylcholine; BK_{Ca}, large-conductance Ca^{2+}-sensitive potassium channel; EDHF, endothelium-derived hyperpolarizing factor; EET, epoxyeicosatrienoic acid; IK_{Ca}, intermediate-conductance Ca^{2+}-sensitive potassium channel; L-NA, N^{ω}-nitro-L-arginine; MβCD, methyl β-cyclodextrin; NS309, 6,7-dichloro-1*H*-indole-2,3-dione 3-oxime; SK_{Ca}, small-conductance Ca^{2+}-sensitive potassium channel; TRAM-34, 1-[(2-chlorophenyl) diphenylmethyl]-1*H*-pyrazole; TRAM-39, 2-(2-chlorophenyl)-2,2-diphenylacetonitrile

Introduction

The endothelium-dependent hyperpolarization and relaxation of vascular myocytes that is independent of the release of nitric oxide and prostacyclin from the vascular endothelium has been widely investigated. In both rat mesenteric and pig coronary arteries, a pivotal feature of this phenomenon, known widely as the endothelium-derived hyperpolarizing factor (EDHF) response, is the opening of endothelial small- and intermediate-conductance Ca^{2+}-sensitive potassium channels (SK_{Ca} and IK_{Ca} respectively; Busse *et al*., 2002; Félétou and Vanhoutte, 2006). Complete inhibition of such endothelium-dependent hyperpolarization (and associated vasorelaxation) triggered by ligands like acetylcholine (ACh), bradykinin and substance P (Alexander *et al*., 2007) can often be achieved by blockade of both IK_{Ca} and SK_{Ca} (Busse *et al*., 2002). However, particularly in coronary and renal vascular beds, the sometimes additional involvement of endothelium-derived epoxyeicosatrienoic acids (EETs) necessitates the supplementary use of an EET-receptor antagonist (Gauthier *et al*., 2002; Weston *et al*., 2005b) or of iberiotoxin.

Correspondence: Dr G Edwards, Faculty of Life Sciences, University of Manchester, 2nd Floor, Core Technology Facility, 46 Grafton Street, Manchester M13 9NT, UK.
E-mail: gillian.edwards@manchester.ac.uk
[3]These authors contributed equally to this work.
Received 4 December 2006; revised 22 January 2007; accepted 5 February 2007; published online 23 April 2007

The toxin blocks the myocyte large-conductance Ca^{2+}-sensitive potassium channels (BK_{Ca}) that are opened by the EETs and which contribute to the observed vasorelaxation in these beds (Weston *et al*., 2005b).

In a study using pig coronary arteries (Graziani *et al*., 2004), it was shown that caveolae might play a role in the bradykinin-activated EDHF response that in these arteries involves not only the activation of SK_{Ca} and IK_{Ca} channels but also the release of EETs (Weston *et al*., 2005b). In these vessels, exposure to methyl β-cyclodextrin (MβCD), an agent known to disrupt caveolae and caveolae-dependent signalling, resulted in a substantial reduction of bradykinin-induced vasorelaxations. Graziani *et al*. (2004) concluded that cholesterol depletion by MβCD had disrupted the integrity of caveolin-rich domains in endothelial cells. They measured an associated reduction in the activity of phospholipase A_2, a key enzyme in the generation of EETs from arachidonic acid.

The objective of the present study was to extend these observations in coronary vessels and to focus on the possible role of caveolin-rich domains in the SK_{Ca}- and IK_{Ca}-mediated components of the EDHF pathway in both porcine coronary and rat mesenteric artery. ACh was used to stimulate this pathway in the rat mesenteric artery, a vessel in which EETs are not involved in the EDHF response (Fukao *et al*., 1997; Vanheel and Van de Voorde, 1997). In parallel experiments, the EDHF pathway in the pig coronary artery was activated using substance P, which, unlike bradykinin (Fisslthaler *et al*., 1999), does not produce EETs in these vessels. Instead, substance P generates an EDHF response that only involves the opening of SK_{Ca} and IK_{Ca} channels (Weston *et al*., 2005b).

Methods

Animals

Experiments were performed on second- and third-order mesenteric artery branches dissected from male Wistar rats (body weight 280–360 g) previously killed by stunning and cervical dislocation in compliance with Schedule 1 of the UK Animals (Scientific Procedures) Act 1986. Pig hearts were obtained from a local abattoir and transported on ice in Krebs solution (mM; 118 NaCl, 3.4 KCl, 1.0 $CaCl_2$, 1.2 KH_2PO_4, 1.2 $MgSO_4$, 25 $NaHCO_3$, 11 glucose, gassed with 5% CO_2, 95% O_2) before dissecting left anterior descending coronary arteries. An identical Krebs solution was used for the rat mesenteric artery studies.

Microelectrode recordings

Membrane potential recordings were performed on intact rat mesenteric artery myocytes and porcine coronary artery endothelial cells as described previously (Weston *et al*., 2005a, b) in the absence of vasoconstrictor drugs. Tissues were constantly superfused with Krebs solution containing 10 μM indomethacin plus 300 μM N^{ω}-nitro-L-arginine (L-NA) at 37°C and gassed with 95% O_2, 5% CO_2. To deplete tissues of cholesterol, 5 mM MβCD was added to the Krebs solution. To restore cholesterol following depletion, the water-soluble cholesterol-PEG 600 (5 mM) was included with the MβCD, as described elsewhere (Shaw *et al*., 2006).

Pressure myography

Second-order mesenteric arteries (approximately 300–350 μm diameter) of 1–2 mm length were cannulated and mounted in a pressure myograph (Living Systems Instrumentation, Burlington, VT, USA) as described previously (Izzard *et al*., 1996). Intraluminal pressure was held at 70 mm Hg and the superfusing Krebs solution contained 300 μM L-NA and 10 μM indomethacin. When appropriate, apamin or 1-[(2-chlorophenyl) diphenylmethyl]-1*H*-pyrazole (TRAM-34) was added to both the superfusate and the luminal solutions. Arteries were preconstricted with an approximate EC_{50} concentration of phenylephrine (5–30 nM). Relaxations to ACh were assessed before and after 45 min incubation with 5 mM MβCD.

Co-localization analysis

Dual labelling of porcine coronary artery sections was achieved using mouse anti-caveolin 1 monoclonal and rabbit anti-SK3, IK1 or eNOS polyclonal primary antibodies with subsequent incubation with species-specific, highly cross-absorbed secondary antibodies. Nuclei were stained with 4′,6-diamidino-2-phenylindole (DAPI) and the internal elastic lamina was visualized using its intrinsic green autofluorescence. Sections were imaged by deconvolution microscopy (DeltaVision system, Issaquah, WA, USA; Applied Precision, USA) in the University of Manchester Imaging Facility. Co-localization analysis of proteins within the endothelium was performed using custom Matlab functions to calculate Pearson's correlation coefficient (r), a value between -1 and $+1$. A value of $+1$ indicated a direct and -1 an inverse relationship between the red and green intensity of a pixel (x and y), with '0' signifying a random distribution.

$$r = \frac{\sum_{i=1}^{n} (x_i - \bar{x})(y_i - \bar{y})}{\sqrt{\sum_{i=1}^{n} (x_i - \bar{x})^2 \sum_{i=1}^{n} (y_i - \bar{y})^2}}$$

A region-of-interest covering the endothelium was defined manually in image stacks (25 slices). Background signal was removed by assigning separate red and green intensity thresholds and excluding pixels with below-threshold intensity in both colour channels. Green signal (caveolin labelling) was similar for all images and the threshold value was set at 2 times the maximum intensity present in unlabelled negative control images. A single threshold was inappropriate for the red signal, which represented anti-SK3, IK1 or eNOS immunoreactivity and so a range of thresholds (2, 4, 6, 8 and 10 times the maximum negative control intensity) was used for each analysis.

Sucrose density gradient ultracentrifugation and Western blotting

Rat mesenteric arteries were subjected to sucrose density gradient ultracentrifugation and Western blotting as described previously (Weston *et al*., 2005a). In initial experiments, the centrifuged sucrose gradient was divided into 13 equal-volume fractions and each fraction analysed by Western blot for the marker proteins caveolin-1 and

β-adaptin. Subsequently, fractions were pooled as fraction 1 (F1), fractions 2–5 (caveolin-rich, C), fractions 6–9 (non-caveolin 1, NC1) and fractions 10–13 (non-caveolin 2, NC2), identical to the previous study (Weston *et al*., 2005a).

Immunoprecipitation

Immunoprecipitation using Dynabeads coupled to goat anti-mouse IgG antibodies was performed by the method of Oh and Schnitzer (1999), except that samples of porcine coronary artery endothelium were prepared in extraction buffer (20 mM Tris, pH 7.5, 250 mM sucrose, 5 mM EDTA, 10 mM EGTA, protease-inhibitor cocktail; P2714, Sigma-Aldrich, Gillingham, UK) and diluted with an equal volume of Tris-buffered saline before homogenization. Samples were analysed by Western blotting as described previously (Burnham *et al*., 2006b).

Statistics

Data, expressed as mean ± s.e.m., were analysed using analysis of variance (ANOVA) (GraphPad Prism software) followed by a Bonferroni post-test, where applicable. A value of $P<0.05$ was considered to be significant.

Drugs and solutions

Antibodies used were anti-SK3 (APC-025; Alomone Laboratories, Jerusalem, Israel), anti-IK1 (a kind gift of Dr M Chen, GlaxoSmithKline), anti-caveolin 1 mAb (clone 2234; BD Transduction Laboratories, San Diego, CA, USA), anti-caveolin 1 pAb (sc-894, Santa Cruz Biotechnology, Santa Cruz, CA, USA) and anti-eNOS (610298, BD Transduction Laboratories). Secondary antibodies were Cy3-conjugated anti-rabbit (Jackson ImmunoResearch, Cambridge, UK) and Alexa 488-conjugated anti-mouse (Molecular Probes, Eugene, OR, USA). Apamin was supplied by Latoxan. *TRAM-34* (1-[(2-chlorophenyl)diphenylmethyl]-1*H*-pyrazole) and TRAM-39 (2-(2-chlorophenyl)-2,2-diphenylacetonitrile) were kind gifts of Dr H Wulff (UC Davis School of Medicine, CA, USA). NS309 (6,7-dichloro-1*H*-indole-2,3-dione 3-oxime) was kindly donated by Dr P Christophersen, NeuroSearch A/S. Cholesterol-PEG 600 (C1145) and all other chemicals were from Sigma-Aldrich (UK).

Results

Rat mesenteric artery microelectrode studies

The smooth-muscle membrane potential in segments of rat mesenteric artery with an intact endothelium was -54.1 ± 0.2 mV ($n=8$) and was unchanged in the presence of 100 nM apamin (-54.3 ± 0.2 mV; $n=4$) or 10 μM TRAM-34 (-54.0 ± 0.2 mV; $n=4$). In the presence of 100 nM apamin (to block endothelial SK_{Ca} channels and reveal responses mediated by IK_{Ca} channels), the peak hyperpolarizations to 1 and 3 μM ACh were similar before (8.7 ± 0.6 and 15.0 ± 0.5 mV, respectively, $n=4$) and after 30 min exposure to 5 mM MβCD (10.1 ± 0.6 and 14.9 ± 0.3 mV, respectively, $n=4$, Figure 1a). The residual ACh-induced hyperpolarizations in the continued presence of apamin and MβCD were abolished by 10 μM TRAM-34, indicating that they were due to the opening of IK_{Ca} channels ($n=4$; data not shown).

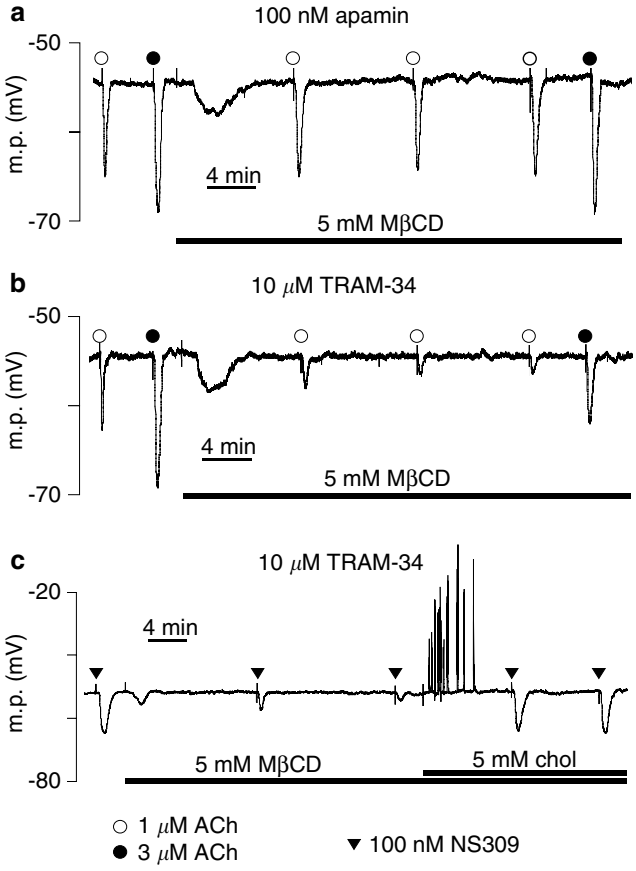

Figure 1 Typical traces showing the effect of MβCD on the SK_{Ca} and IK_{Ca}-induced myocyte hyperpolarizations in rat mesenteric artery segments. MβCD had no effect on (**a**, presence of apamin) the IK_{Ca} component of the response to ACh (**b**, presence of TRAM-34) but markedly reduced the SK_{Ca} component. (**c**, presence of TRAM-34) Similarly, the SK_{Ca} component of the hyperpolarization to NS 309 was also reduced by MβCD, an effect that was reversed by simultaneous exposure to cholesterol (chol).

In the presence of 10 μM TRAM-34 (to block endothelial IK_{Ca} channels and reveal responses mediated by SK_{Ca} channels), peak hyperpolarizations to both 1 and 3 μM ACh (8.2 ± 0.4 and 14.6 ± 0.5 mV, respectively, $n=4$) were similar to those in the presence of 100 nM apamin. In contrast, however, both were significantly reduced by 30 min MβCD treatment (2.3 ± 0.2 and 6.1 ± 0.5 mV, respectively; $P<0.001$, two-way ANOVA $n=4$, Figure 1b).

To determine whether the inhibitory effects of MβCD on ACh-induced, SK_{Ca}-mediated hyperpolarizations (Figure 1b) somehow involved an action on the endothelial muscarinic receptors, vessels were exposed to 100 nM NS309 (a direct opener of both IK_{Ca} and SK_{Ca} channels; Strøbæk *et al*., 2004) in the presence of the IK_{Ca} blocker TRAM-34 (10 μM). Under these conditions, NS309 hyperpolarized mesenteric artery myocytes by 13.2 ± 0.3 mV ($n=4$). MβCD (5 mM) time dependently reduced this hyperpolarization (to 7.4 ± 0.9 mV after 15 min and to 3.9 ± 0.5 mV after 30 min, $n=4$), effects that were reversed by subsequent inclusion of 5 mM cholesterol-PEG 600 (hyperpolarizations to NS309 were

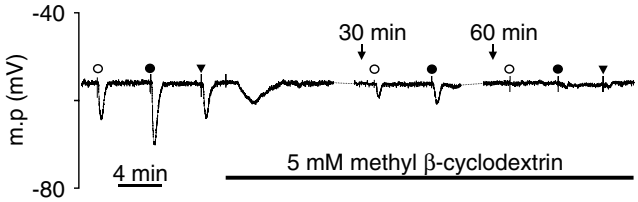

Figure 2 Typical trace showing the effect of prolonged MβCD treatment on SK_{Ca}-dependent responses in rat mesenteric artery. Myocyte membrane potential was continuously recorded in the presence of TRAM-34. Responses to ACh were reduced after 30 min treatment with MβCD and these residual responses were essentially abolished by a further 30 min incubation with MβCD, as were responses to NS 309. Symbols used are identical to those in Figure 1. The broken lines in the membrane potential record indicate where a portion has been omitted for clarity; the cell remained impaled by the electrode.

11.2 ± 0.5 mV after 10 min and 13.9 ± 0.1 mV after 20 min exposure to cholesterol-PEG 600 in the presence of MβCD, $n = 4$, Figure 1c).

A further series of experiments was undertaken to determine whether the small residual SK_{Ca}-dependent hyperpolarizations recorded after 30 min MβCD treatment represented a genuine MβCD-resistant component of the response or were the result of the relatively short exposure to MβCD. Responses to 1 and 3 μM ACh in the presence of 10 μM TRAM-34 were recorded before MβCD treatment and again in the same arteries after 30 and 60 min incubation with 5 mM MβCD ($n = 4$; Figure 2). Before MβCD treatment, ACh (1 and 3 μM) produced hyperpolarizations of 8.3 ± 1.0 and 16.3 ± 1.4 mV, respectively. These responses were reduced to 2.3 ± 0.3 and 7.2 ± 1.4 mV after 30 min treatment and essentially abolished after 60 min exposure to MβCD (0.0 ± 0.0 and 1.5 ± 0.6 mV). In two of these experiments, responses to 100 nM NS309 were also determined. The mean hyperpolarization of 9.3 mV recorded before MβCD treatment was reduced to 0.7 mV after 60 min.

Porcine coronary artery microelectrode studies

To extend the data to more than one species and, additionally, to exclude the possibility that MβCD exerted its effects on the coupling between endothelium and smooth muscle, membrane potential recordings were obtained directly from the endothelium of porcine coronary arteries. The mean basal membrane potential of porcine coronary artery endothelial cells before the start of experimentation was -51.2 ± 4.1 mV ($n = 8$). In the presence of 100 nM apamin to block endothelial SK_{Ca} channels, their resting membrane potential was -50.6 ± 0.3 mV ($n = 4$). Control hyperpolarizations were first recorded to 100 nM substance P (21.3 ± 0.6 mV); on superfusion with 1 mM MβCD, responses to substance P were not significantly different from controls after 10 min (20.4 ± 1.0 mV), 20 min (19.9 ± 1.0 mV) or 30 min (20.2 ± 0.9 mV), whereas additional application of 10 μM TRAM-39 abolished substance P responses (0.3 ± 0.1 mV; $n = 3$).

The above protocol was repeated in fresh tissue segments ($n = 4$) with 10 μM TRAM-39 (in place of apamin) to block IK_{Ca} channels leaving only SK_{Ca} channels available for activation by substance P. From a basal membrane potential of -50.4 ± 0.1 mV, mean control hyperpolarizations of endothelial cells to substance P were 20.0 ± 1.9 mV. On superfusion with MβCD, substance P responses were significantly reduced after 10 min (13.2 ± 3.6 mV) and further reduced at 20 (7.3 ± 1.7 mV) and 30 min (6.3 ± 2.0 mV). Subsequent application of 100 nM apamin in the continuing presence of MβCD effectively abolished the residual substance P hyperpolarizations (0.2 ± 0.0 mV; $n = 3$).

Pressure myography

The mean diameter of rat mesenteric arteries used for pressure myography was 326 ± 15 μm ($n = 16$). In the presence of 100 nM apamin to block SK_{Ca} channels, 1 and 3 μM ACh relaxed a phenylephrine-induced contraction by 84 ± 8 and 93 ± 2%, respectively ($n = 4$). Following 5 mM MβCD treatment for 40 min, relaxations to 1 and 3 μM ACh were unaffected (79 ± 8 and 89 ± 10%, respectively, $n = 4$, Figure 3a). In separate artery segments in the presence of 10 μM TRAM-34 to block IK_{Ca} channels, 1 and 3 μM ACh relaxed phenylephrine contractions by 46 ± 5 and 78 ± 8%, respectively ($n = 4$). After MβCD treatment for 40 min, relaxations to both 1 and 3 μM ACh were significantly reduced (to 7 ± 3 and 16 ± 6%, respectively; two-way ANOVA, $P < 0.001$, $n = 4$, Figure 3b).

Sucrose-density gradient fractionation

In the present study, the distribution of the proteins caveolin-1 (caveolae-associated marker) and β-adaptin (non-caveolae marker; Sampson *et al*., 2004) were determined in the unpooled sucrose gradient fractions and a clear differentiation was observed (Figure 4a). When the fractions, pooled as described in the Methods section, were analysed for SK3 and IK1 protein, a distinct pattern was observed under control conditions (Figure 4b), as previously reported (Weston *et al*., 2005a). The SK3 protein migrated with caveolin-1 into the lipid-rich fractions, whereas IK1 was retained in the dense, non-caveolin fractions. However, when rat mesenteric arteries were pretreated with 5 mM MβCD for 30 min, significant amounts of both caveolin and SK3 protein were present in all fractions, but predominantly in the higher-density fractions rather than the caveolin-rich (C) fraction only. In contrast, MβCD treatment failed to affect the distribution of IK1 protein, which remained predominantly in the high-density fractions (Figure 4b). To demonstrate antibody specificity, Western blotting experiments were performed with lysates of transfected human embryonic kidney (HEK) cells and these experiments confirmed that anti-SK3 and -IK1 immunoreactivity was limited to samples of SK3- and IK1-transfected cells, respectively (Figure 4c). Aggregation of subunit proteins may underlie the high molecular weight smearing observed (Soulie *et al*., 1996).

Deconvolution microscopy and image analysis

Antibody specificity control experiments with HEK cells expressing SK3 or IK1 proteins indicated that both anti-SK3 and -IK1 antibodies labelled only those cells containing the

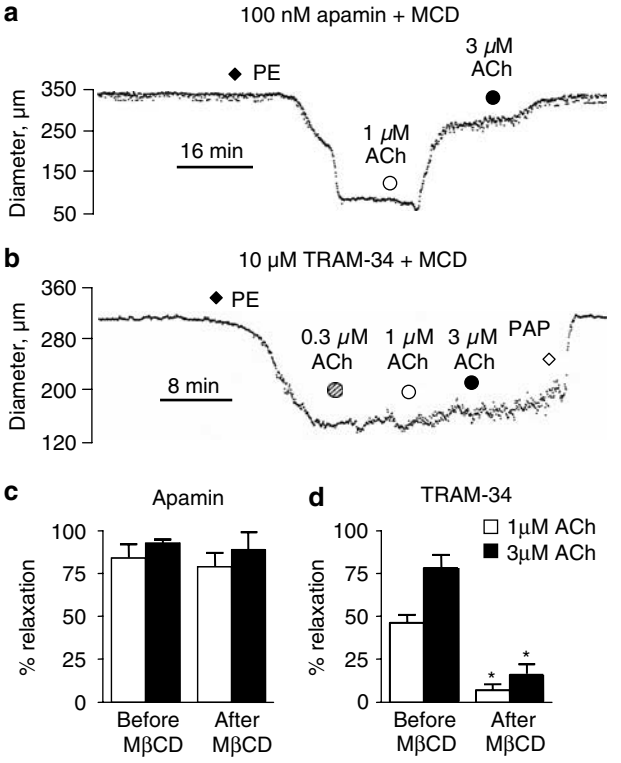

Figure 3 Typical traces showing the effect of MβCD on IK_{Ca}- and SK_{Ca}-dependent vasorelaxation in rat mesenteric arteries. Arteries were mounted on a pressure myograph and pressurized to 70 mm Hg. Arteries were pre-incubated for 45 min with 5 mM MβCD and either (**a**) 100 nM apamin or (**b**) 10 μM TRAM-34. Arteries were constricted with 5–30 nM phenylephrine (PE) and 0.3–3 μM ACh applied. Full relaxation was induced with 100 μM papaverine. Mean data showing relaxations to ACh in the presence of (**c**) apamin and (**d**) TRAM-34 before and after incubation with MβCD ($n=4$).

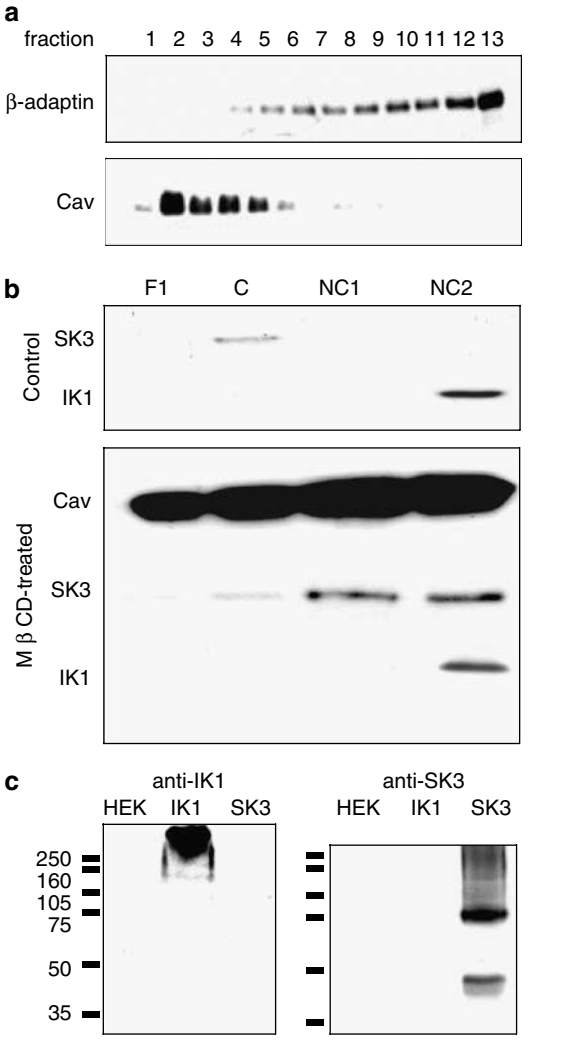

Figure 4 (**a**) Sucrose density gradient fractions analysed by Western blot for the presence of caveolin-1 (Cav) and β-adaptin protein (a non-caveolae marker). Subsequently, fractions were pooled as fraction 1 (F1), fractions 2–5 (caveolin-rich, C), fractions 6–9 (non-caveolin 1, NC1) and fractions 10–13 (non-caveolin 2, NC2). (**b**) Effect of MβCD on SK3, IK1 and caveolin-1 protein distribution. Arteries were incubated with 5 mM MβCD for 30 min (lower panel) or left untreated (upper panel) before subjecting the resultant sucrose density gradient fractions to Western blotting. Note the migration of the SK3 and caveolin proteins into the NC fractions on MβCD treatment. (**c**) Western blot analysis showing the specificity of the anti-IK1 and anti-SK3 antibodies used in the sucrose density gradient experiments shown in (**b**) above. Note that each antibody recognizes only protein in HEK cells transfected with the appropriate subunit and does not react with any proteins in either untransfected HEK cells or those transfected with the alternative subunit. Molecular weight markers (kDa) are indicated. Images representative of three separate experiments are shown.

appropriate subunit and that the antibodies did not cross-react with the other subunit or with other HEK cell proteins (Figure 5a). Sections of porcine coronary artery labelled with anti-IK1 antibodies displayed strong endothelial immunoreactivity that was prevented by pre-incubation of the antibody with immunogenic peptide (Figure 5a). Weaker labelling that was not blocked by immunogenic peptide pre-incubation was visible in the smooth muscle. Previous experiments have shown that anti-SK3 immunoreactivity is restricted to the endothelium in this tissue (Burnham *et al*., 2002).

Co-localization of caveolin-1 with IK1, SK3 or eNOS proteins within the endothelium was determined by co-labelling of porcine coronary sections followed by deconvolution microscopy and image analysis (Figures 5b and c). Vertical spacing within a 25-image stack was 0.2 μm, indicating that an individual caveola <100 nm in diameter (Gratton *et al*., 2004) would not appear on consecutive images. Co-localization (Pearson's correlation coefficient *r*, determined across a range of background thresholds) was positive for caveolin and SK3 and this parameter was not significantly different when calculated for caveolin and eNOS, a protein known to be associated with caveolae (Garcia-Cardena *et al*., 1996; Shaul *et al*., 1996). However, caveolin/IK1 co-localization was negative and significantly different from caveolin/eNOS and caveolin/SK3, strongly suggesting that IK1 was not spatially associated with caveolin in the manner of eNOS or SK3.

Immunoprecipitation

Anti-caveolin-1 immunoprecipitates prepared from homogenates of porcine coronary artery endothelium were

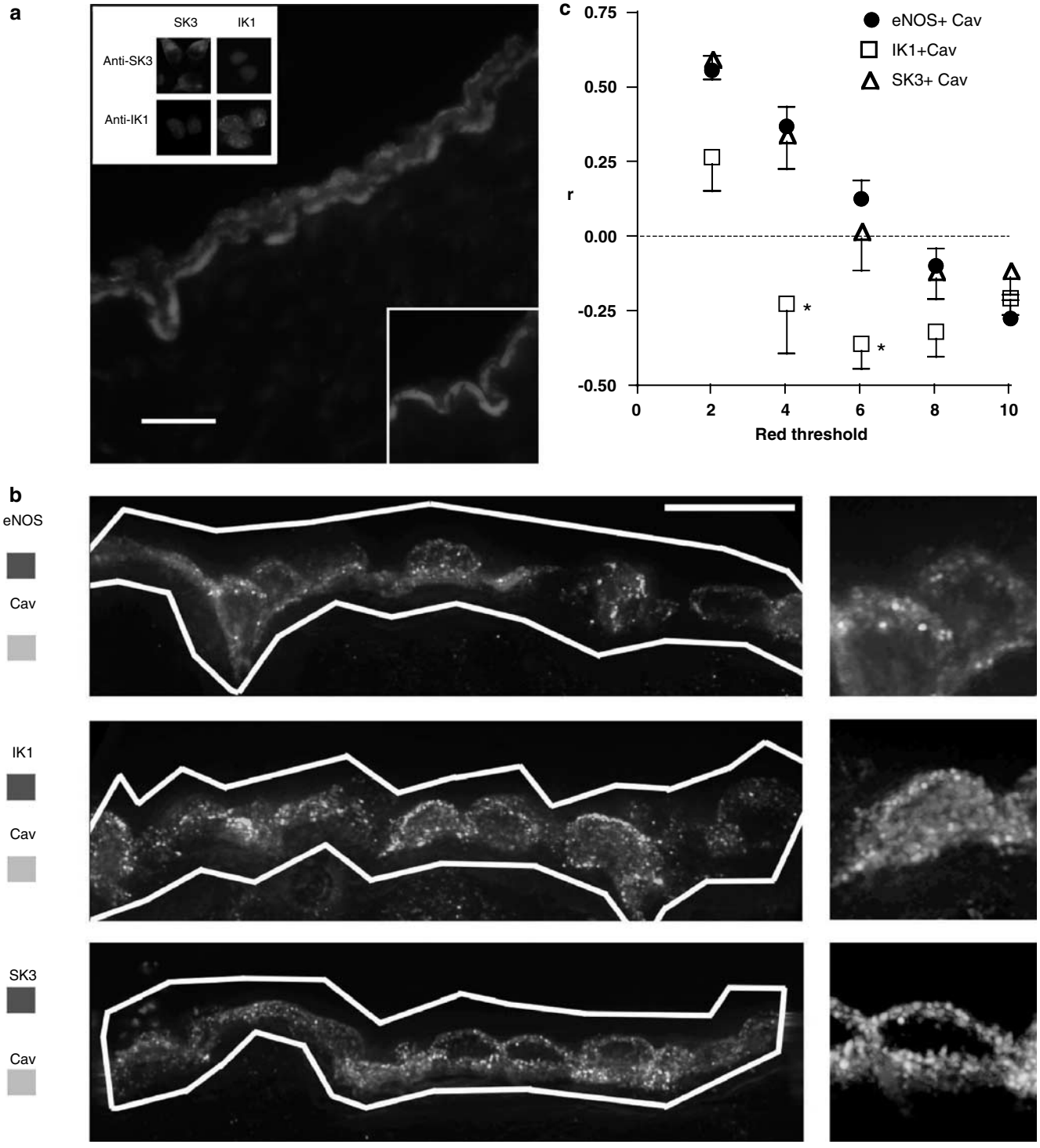

Figure 5 (**a**) Detection and localization of IK1 in sections of porcine coronary artery. Anti-IK1 immunoreactivity (red), nuclei (blue) and internal elastic lamina (green) are shown (representative of $n=4$ animals). All scale bars are 12.5 μm. Negative control experiment with anti-IK1 antibody pre-incubated with antigenic peptide (inset bottom right). Antibody specificity control data showing HEK cells expressing SK3 and IK1 immunolabelled with anti-SK3 and anti-IK1 antibodies (inset top left; representative of three separate experiments). (**b**) Deconvolution microscopy images of porcine coronary artery sections co-labelled with anti-caveolin-1 (Cav) and anti-eNOS, anti-IK1 or anti-SK3 antibodies. Low and high power magnification images shown are histogram-equalized z-projections of 25-image stacks. White lines enclose endothelial areas included in the co-localization analysis. (**c**) Graph of co-localization analysis mean data (eNOS, $n=100$ images, four animals; SK3, IK1, $n=75$ images, three animals) showing Pearson's correlation coefficient (r) versus red threshold for anti-eNOS, SK3 or IK1 with anti-caveolin-1 immunoreactivity ($r=+1$ indicates perfect co-localization, $r=0$ indicates no correlation and $r=-1$ indicates perfect negative correlation). (For colour figure see online version.)

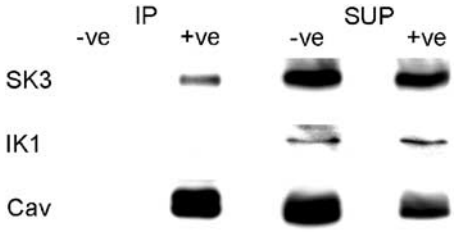

Figure 6 Anti-SK3, IK1 and caveolin-1 Western blot analysis of anti-caveolin-1 immunoprecipitates prepared from porcine coronary artery endothelium. Immunoprecipitation (IP) was performed with and without anti-caveolin-1 antibody (+ve and −ve, respectively). Supernatants remaining after IP (SUP) were also subjected to Western blot analysis. Note that the SK3 protein co-precipitates with the caveolin-1 protein, whereas the IK1 protein does not. Images are representative of five (SK3) and three (IK1) experiments.

analysed by anti-SK3, -IK1 and -caveolin-1 Western blotting (Figure 6). Caveolin-1 protein was robustly detected in immunoprecipitates and this was accompanied by a reduction in caveolin protein in unbound supernatants. Anti-caveolin immunoprecipitates also contained SK3 protein ($n=5$), whereas IK1 protein was only detected in unbound supernatants ($n=3$). As a control for non-specific binding, the immunoprecipitation procedures were performed without anti-caveolin-1 antibody and no signal was detected upon Western blotting.

Discussion

The aim of the present study was to investigate the importance of caveolin-rich domains in EDHF-mediated responses involving K_{Ca} channels in both rat and porcine blood vessels with the primary objective of learning more about the intracellular organization of the EDHF-signalling cascade. The results show that in both vascular beds, there is a fascinating difference between the location of the endothelial SK_{Ca} and IK_{Ca} channels that play a pivotal role in the EDHF response. Although the functional evidence is critically dependent on the results obtained with the cholesterol-depleting agent MβCD, these data, when combined with the results from imaging and other biochemical approaches obtained independently of MβCD, all indicate that SK_{Ca} channels reside within caveolin-rich lipid domains (almost certainly caveolae) rather than in lipid rafts and that this position within the cell is one that they do not share with IK_{Ca}.

Rat mesenteric artery

The general strategy adopted was first to isolate the SK_{Ca} and IK_{Ca} components of agonist-induced EDHF responses using TRAM-34 or apamin, respectively, and then to employ MβCD as the cholesterol-depleting agent. Thus, in the presence of TRAM-34 and following treatment with MβCD over a 30 min period, the SK_{Ca} component of the endothelium-dependent hyperpolarization to ACh became markedly reduced. In contrast, after isolating the ACh-induced, IK_{Ca}-mediated hyperpolarization using apamin, exposure to MβCD over a 30 min period had no significant effect on responses to ACh. This finding was reproduced in the pressure myograph experiments in which treatment with MβCD reduced only the SK_{Ca}-mediated EDHF-dependent dilation of rat mesenteric arteries.

Such selective impairment by MβCD of the SK_{Ca} component of the EDHF response could have resulted if the coupling between muscarinic-receptor activation and SK_{Ca} opening involved a mechanism not shared by the muscarinic receptor – IK_{Ca} interaction. To clarify this, we employed NS309, an opener of both IK_{Ca} and SK_{Ca} channels by a mechanism independent of muscarinic receptor activation (Strøbæk *et al*., 2004). In these experiments, the selective NS309-induced opening of SK_{Ca} channels seen in the presence of TRAM-34 was also markedly reduced by MβCD. Thus, the ability of MβCD to modify the SK_{Ca} component of both ACh- and NS309-induced K_{Ca} channel opening shows that the action of MβCD is not exerted on the muscarinic receptor but rather on the SK_{Ca} channel itself. Significantly, the reduction in the SK_{Ca}-mediated component was rapidly reversed by the inclusion of cholesterol in the bathing medium. Collectively, these data strongly suggest that cholesterol depletion by MβCD in rat mesenteric vessels selectively impairs the activation of SK_{Ca} channels. From this, it can be inferred that these are probably located in caveolae or lipid rafts in marked contrast to the IK_{Ca} channels that are not associated with these structures.

Porcine coronary artery

The EDHF response has been widely studied in the porcine coronary artery, often using the local hormone bradykinin to activate the system (Fisslthaler *et al*., 1999). In this vascular bed, the bradykinin-induced EDHF response is more complex than in some other vessels as this agent not only activates IK_{Ca} and SK_{Ca} channels but also stimulates the production of 11,12- and 14,15-EET. These then subsequently activate endothelial IK_{Ca} and SK_{Ca} channels and also BK_{Ca} channels on the vascular myocytes (Weston *et al*., 2005b). To avoid these complexities, substance P acting via NK1 receptors (Alexander *et al*., 2007) was used to activate the pathway. In porcine coronary arteries, substance P produces an EDHF response which results solely from the opening of IK_{Ca} and SK_{Ca} channels and which is independent of the production of EETs (Weston *et al*., 2005b).

Consistent with the findings in the rat mesenteric artery, porcine coronary artery endothelial cell hyperpolarizations to substance P which were elicited through SK_{Ca} channels alone (i.e., in the presence of TRAM-39) were attenuated following exposure to MβCD, whereas IK_{Ca}-mediated hyperpolarizations (in the presence of apamin) were unaffected. The sustained IK_{Ca}-mediated response in the presence of MβCD is a strong indication that substance P receptors were neither desensitized nor uncoupled from downstream effectors during MβCD treatment. In addition, the fact that microelectrode recordings were made from the endothelial cells of these arteries (as opposed to the measurements from myocytes in the rat mesenteric artery study) means that the reduction in SK_{Ca}-mediated hyperpolarizations did not reflect an inhibitory action on endothelium–myocyte coupling processes.

Molecular studies

To consolidate the electrophysiological findings, the subcellular distributions of the SK_{Ca} and IK_{Ca} channel-forming proteins SK3 and IK1, respectively, were investigated. In rat mesenteric arteries treated with MβCD, sucrose-density gradient experiments showed that both caveolin-1 and SK3 immunoreactivities were redistributed across a range of density fractions, whereas in untreated arteries both caveolin-1 and SK3 proteins were restricted to the buoyant caveolin-rich fraction. Thus, it appears that the presence of SK3 in the buoyant fraction may be dependent on intact caveolae and/or lipid rafts, whereas the occurrence of IK1 in denser fractions is cholesterol-independent.

From these studies with MβCD, it can be concluded that membranes rich in cholesterol (e.g., lipid rafts or caveolae) harboured the SK3 protein and that MβCD treatment disrupted these membranes and hence SK3 localization through a cholesterol-depleting mechanism. To delineate more clearly the cellular location of SK3, further studies were conducted using freshly-isolated native endothelial cells from the porcine coronary artery. In deconvolved immunofluorescence images, the co-localization of SK3 and caveolin-1 immunoreactivities occurred to a degree similar to that observed between caveolin-1 and eNOS (a known caveolae-associated protein; Garcia-Cardena *et al*., 1996; Shaul *et al*., 1996). Additionally, a physical interaction between SK3 and caveolin-1 was demonstrated by the presence of SK3 in caveolin immunoprecipitates. This close association between SK3 and caveolin is consistent with the localization of SK_{Ca} channels within caveolae rather than with lipid rafts. In contrast, IK1 was not physically associated with caveolin-1 and these two proteins apparently occupy distinct membrane compartments. Collectively, these findings are entirely consistent with the electrophysiological data. They strengthen the view that the endothelial SK_{Ca} channels so important in the EDHF response are located in caveolae, a location not shared by the IK_{Ca} channels.

Conclusions

The findings of the present study have shown that in two dissimilar vascular beds, the endothelial SK_{Ca} channels are located in caveolin-rich domains, whereas IK_{Ca} is found in a different cellular fraction not associated with either caveolin or MβCD-sensitive lipid rafts. The present results in porcine coronary vessels show the importance of caveolae in generating not only the SK_{Ca} component of the EDHF response but, when combined with the results of earlier investigators (Haasemann *et al*., 1998; Graziani *et al*., 2004), also in the production of EETs. In the rat mesenteric bed, the different locations of the endothelial SK_{Ca} and IK_{Ca} channels appear identical to those in the porcine coronary vessels. These differences may go some way to explain the recently-reported selective impairment of the SK_{Ca}-mediated component of EDHF responses in the Zucker diabetic fatty rat (Burnham *et al*., 2006a).

The list of membrane proteins that are associated with caveolin/caveolae is growing rapidly (Frank *et al*., 2003) and it is thus remarkable that the IK1 protein does not share the same location as the SK3 protein with which it is mechanistically linked in the EDHF cascade. However, it is not alone in this respect as a recent study (Weston *et al*., 2005a; also in rat and porcine vessels) has shown that the extracellular Ca^{2+}-sensing receptor is also not associated with the caveolin-rich domains. Further studies are in progress to clarify how the IK_{Ca} channel, in contrast to SK_{Ca}, can function outside a microdomain that is so important in facilitating the interactions between receptors, channels and signalling mechanisms.

Acknowledgements

We acknowledge the support of the University of Aleppo, Syria (MA), the British Heart Foundation (Grants PG/05/058, PG/05/010; MB, GE, AHW) and the Royal Society (GE) for supporting this work. We thank Dr H Wulff (UC Davis School of Medicine, CA) and Dr P Christophersen (NeuroSearch A/S) for TRAM and NS309 compounds, respectively, and the staff of the abattoir (Steve, Alan and Howard).

Conflict of interest

The authors state no conflict of interest.

References

Alexander SPH, Mathie A, Peters JA (2007). Guide to receptors and channels (GRAC), 2nd edition (2007 revision). *Br J Pharmacol* **150** (Suppl 1): S1–S168.

Burnham MP, Bychkov R, Félétou M, Richards GR, Vanhoutte PM, Weston AH *et al*. (2002). Characterization of an apamin-sensitive small-conductance Ca^{2+}-activated K^+ channel in porcine coronary artery endothelium: relevance to EDHF. *Br J Pharmacol* **135**: 1133–1143.

Burnham MP, Johnson IT, Weston AH (2006a). Impaired small-conductance Ca^{2+}-activated K^+ channel-dependent EDHF responses in Type II diabetic ZDF rats. *Br J Pharmacol* **148**: 434–441.

Burnham MP, Johnson IT, Weston AH (2006b). Reduced Ca^{2+}-dependent activation of large-conductance Ca^{2+}-activated K^+ channels from arteries of Type 2 diabetic Zucker diabetic fatty rats. *Am J Physiol* **290**: H1520–H1527.

Busse R, Edwards G, Félétou M, Fleming I, Vanhoutte PM, Weston AH (2002). EDHF: bringing the concepts together. *Trends Pharmacol Sci* **23**: 374–380.

Félétou M, Vanhoutte PM (2006). Endothelium-derived hyperpolarizing factor. Where are we now? *Arterioscler Thromb Vasc Biol* **26**: 1215–1225.

Fisslthaler B, Popp R, Kiss L, Potente M, Harder DR, Fleming I *et al*. (1999). Cytochrome P450 2C is an EDHF synthase in coronary arteries. *Nature* **401**: 493–497.

Frank PG, Woodman SE, Park DS, Lisanti MP (2003). Caveolin, caveolae, and endothelial cell function. *Arterioscler Thromb Vasc Biol* **23**: 1161–1168.

Fukao M, Hattori Y, Kanno M, Sakuma I, Kitabatake A (1997). Evidence against a role of cytochrome P450-derived arachidonic acid metabolites in endothelium-dependent hyperpolarization by acetylcholine in rat isolated mesenteric artery. *Br J Pharmacol* **120**: 439–446.

Garcia-Cardena G, Fan R, Stern DF, Liu J, Sessa WC (1996). Endothelial nitric oxide synthase is regulated by tyrosine phosphorylation and interacts with caveolin-1. *J Biol Chem* **271**: 27237–27240.

Gauthier KM, Deeter C, Krishna UM, Reddy YK, Bondlela M, Falck JR *et al*. (2002). 14,15-Epoxyeicosa-5(Z)-enoic acid: a selective epoxyeicosatrienoic acid antagonist that inhibits endothelium-

dependent hyperpolarization and relaxation in coronary arteries. *Circ Res* **90**: 1028–1036.

Gratton JP, Bernatchez P, Sessa WC (2004). Caveolae and caveolins in the cardiovascular system. *Circ Res* **94**: 1408–1417.

Graziani A, Bricko V, Carmignani M, Graier WF, Groschner K (2004). Cholesterol- and caveolin-rich membrane domains are essential for phospholipase A_2-dependent EDHF formation. *Cardiovasc Res* **64**: 234–242.

Haasemann M, Cartaud J, Muller-Esterl W, Dunia I (1998). Agonist-induced redistribution of bradykinin B2 receptor in caveolae. *J Cell Sci* **111**: 917–928.

Izzard AS, Bund SJ, Heagerty AM (1996). Myogenic tone in mesenteric arteries from spontaneously hypertensive rats. *Am J Physiol* **270**: H1–H6.

Oh P, Schnitzer JE (1999). Immunoisolation of caveolae with high affinity antibody binding to the oligomeric caveolin cage. Toward understanding the basis of purification. *J Biol Chem* **274**: 23144–23154.

Sampson LJ, Hayabuchi Y, Standen NB, Dart C (2004). Caveolae localize protein kinase A signaling to arterial ATP-sensitive potassium channels. *Circ Res* **95**: 1012–1018.

Shaul PW, Smart EJ, Robinson LJ, German Z, Yuhanna IS, Ying Y *et al*. (1996). Acylation targets endothelial nitric-oxide synthase to plasmalemmal caveolae. *J Biol Chem* **271**: 6518–6522.

Shaw L, Sweeney MA, O'Neill SC, Jones CJ, Austin C, Taggart MJ (2006). Caveolae and sarcoplasmic reticular coupling in smooth muscle cells of pressurised arteries: the relevance for Ca^{2+} oscillations and tone. *Cardiovasc Res* **69**: 825–835.

Soulie S, Moller JV, Falson P, le Maire M (1996). Urea reduces the aggregation of membrane proteins on sodium dodecyl sulfate-polyacrylamide gel electrophoresis. *Anal Biochem* **236**: 363–364.

Strøbæk D, Teuber L, Jorgensen TD, Ahring PK, Kjaer K, Hansen RS *et al*. (2004). Activation of human IK and SK Ca^{2+} -activated K^+ channels by NS309 (6,7-dichloro-1*H*-indole-2,3-dione 3-oxime). *Biochim Biophys Acta* **1665**: 1–5.

Vanheel B, Van de Voorde J (1997). Evidence against the involvement of cytochrome P450 metabolites in endothelium-dependent hyperpolarization of the rat main mesenteric artery. *J Physiol* **501**: 331–341.

Weston AH, Absi M, Ward DT, Ohanian J, Dodd RH, Dauban P *et al*. (2005a). Evidence in favor of a calcium-sensing receptor in arterial endothelial cells: studies with calindol and Calhex 231. *Circ Res* **97**: 391–398.

Weston AH, Félétou M, Vanhoutte PM, Falck JR, Campbell WB, Edwards G (2005b). Bradykinin-induced, endothelium-dependent responses in porcine coronary arteries: involvement of potassium channel activation and epoxyeicosatrienoic acids. *Br J Pharmacol* **145**: 775–784.